MedChemComm

Accepted Manuscript

This is an *Accepted Manuscript*, which has been through the Royal Society of Chemistry peer review process and has been accepted for publication.

Accepted Manuscripts are published online shortly after acceptance, before technical editing, formatting and proof reading. Using this free service, authors can make their results available to the community, in citable form, before we publish the edited article. We will replace this *Accepted Manuscript* with the edited and formatted *Advance Article* as soon as it is available.

You can find more information about *Accepted Manuscripts* in the Information for Authors.

Please note that technical editing may introduce minor changes to the text and/or graphics, which may alter content. The journal's standard Terms & Conditions and the Ethical guidelines still apply. In no event shall the Royal Society of Chemistry be held responsible for any errors or omissions in this *Accepted Manuscript* or any consequences arising from the use of any information it contains.

ROYAL SOCIETY OF CHEMISTRY

www.rsc.org/medchemcomm

Discovery of Pyridyl-based inhibitors of *Plasmodium falciparum* *N*-myristoyltransferase

Zhiyong Yu[†△], *James A. Brannigan*[‡], *Kaveri Rangachari*[§], *William P. Heal*[†,&], *Anthony J. Wilkinson*[‡], *Anthony A. Holder*,[§] *Robin J. Leatherbarrow*[†$] *and Edward W. Tate*[†]*

[†] Department of Chemistry, Imperial College London, London, SW7 2AZ, U.K.

[‡] York Structural Biology Laboratory, Department of Chemistry, University of York, York, YO10 5DD, U.K.

[§] The Francis Crick Institute, Mill Hill Laboratory, The Ridgeway, London, NW7 1AA, U.K.

[△]Current address: International Discovery Service Unit, WuXi AppTec, Shanghai, 200131, China

[&] Current address: Department of Chemistry, Kings College London, London SE1 1UL, UK.

[$]Current address: Egerton Court, Liverpool John Moores University, Liverpool L1 2UA, UK

ABSTRACT

N-myristoyltransferase (NMT) represents an attractive drug target in parasitic infections such as malaria due to its genetic essentiality and amenability to inhibition by drug-like small molecules. Scaffold simplification from previously reported inhibitors containing bicyclic cores identified phenyl derivative **3**, providing a versatile platform to study the effects of substitution on the scaffold, which yielded pyridyl **19**. This molecule exhibited improved enzyme and cellular potency, and reduced lipophilicity compared to inhibitor **3**. Further structure-based inhibitor design led to the discovery of **30**, the most potent inhibitor in this series, which showed single-digit nM enzyme affinity and sub-μM anti-plasmodial activity.

INTRODUCTION

Malaria, a parasitic disease in humans primarily caused by *Plasmodium falciparum* (Pf) and *Plasmodium vivax* (Pv), was responsible for about 584,000 deaths in 2013, mainly of pregnant women and children living in Africa.[1] Recent vaccine trials have met with moderate success[2, 3]. However, the first signs of resistance to artemisinin, currently the first-line antimalarial treatment, have emerged in Southeast Asia.[4-6] It is therefore important to develop new antimalarial medications with novel modes of action.[7]

N-myristoyltransferase (NMT) is an enzyme ubiquitous in eukaryotes, catalysing co- or post-translational transfer of myristate (C14:0 fatty acid) from myristoyl-coenzyme A (myr-CoA) to the N-terminal glycine of a subset of eukaryotic proteins.[8-12] In *Plasmodium*, numerous essential proteins have been shown to require

myristoylation to fulfil their biological functions.[13-18] The essentiality and druggability of NMT has been demonstrated in blood stage *P. falciparum*,[19] and in the closely related rodent pathogen *P. berghei*.[20] We recently reported the discovery of several novel series of small molecule parasitic NMT inhibitors,[19, 21-24] in addition to peptidomimetic inhibitors.[25] To date, development of these series has focused on inhibitors containing bicyclic aromatic cores.[26-28] In two complementary studies, we report the design and development of a simplified single ring scaffold, which provides a more flexible platform to study substitution patterns on the aromatic core and has enabled targeting of both plasmodial and leishmanial NMTs.[29] Crystal structures of these inhibitors in complex with NMT enabled Structure-Activity Relationships (SARs) to be derived; this report describes the discovery of a new highly potent *P. falciparum* NMT (PfNMT) inhibitor that is active against parasites, and with promising selectivity relative to human NMTs and human cell lines.[24]

RESULTS AND DISCUSSION

Following the discovery that single-ring scaffolds displayed good affinity against *Leishmania donovani* NMT,[29] disubstituted (*ortho*-and *meta*-) phenyl rings were selected as analogues of the structures of previously reported inhibitors **1** and **2**,[27, 28] and linked through an ester or its bioisosteric oxadiazole to a terminal benzyl substituent (Figure 1). Among the four different combinations (Table S1, Supporting Information), compound **3** was found to display comparable enzyme potency and human selectivity to the bicyclic equivalents (Figure 1).

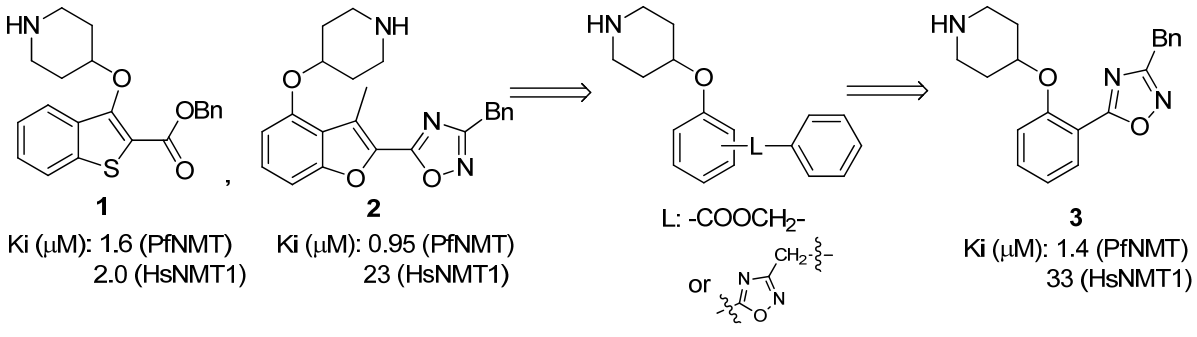

Figure 1. Scaffold hopping from previously described inhibitors **1** and **2** containing a bicyclic aromatic core [27, 28] to identify phenyl **3** as a starting compound.

Variation of the single ring core. A library of compounds (**4-17**) with varied substitutions on the single ring scaffold was synthesised (scheme 1). Initial ester protection of salicylic acid analogues enabled the incorporation of an *N*-Boc piperidinol side chain into the scaffold via a Mitsunobu reaction, followed by hydrolysis of the ester to form the corresponding carboxylic acid intermediate (**4b-17b**). The final 1,2,4-oxadiazole compounds were then synthesized using a modification of previously-reported conditions.[28]

Scheme1[a]

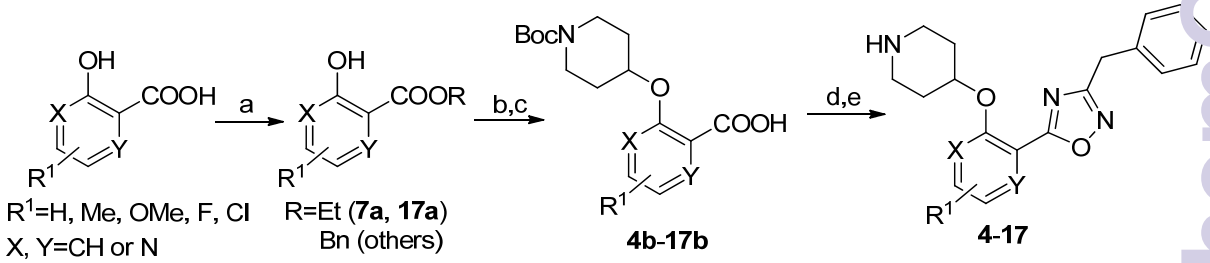

[a]Reagents: (a) BnBr, K_2CO_3, DMF, rt, 2 h, 86%; as for **7a**, i). $SOCl_2$, 90˚C, 1h; ii) EtOH, rt, 1 h, 95%; as for **17a**, H_2SO_4, EtOH/benzene, 80˚C, 2 h, 70%; (b) DIAD,

PPh_3, *t*-butyl 4-hydroxypiperidine-1-carboxylate, THF, rt, 4 h; (c)NaOH, MeOH/H_2O, 50°C, 2 h, quantitative over two steps; (d) i). benzylamidoxime, EDCI, HOBt, DIPEA, CH_3CN, rt, 4 h; ii). 0.5N NaOH, rt, 0.5h, 90%; (e) 10% TFA in DCM (v/v), rt, 2h, quantitative.

The biological activities of these compounds are detailed in Table 1. Substitution at C-3 was disfavored for inhibition of PfNMT (**4** and **5** vs. **3**, Table 1), with only fluorine (**6**) tolerated at this position by the enzyme. However, the 3-pyridyl analogue of **3** exhibited both reduced lipophilicity and a 10-fold improvement in enzyme affinity (**7** vs. **3**). Within the phenyl series, substitution at the C-4 position generally enhanced enzyme inhibition, with methyl (**8** vs. **3**) somewhat less effective than halogen (**10**, **11** vs. **3**) or methoxy (**9**), with minor variations in selectivity over the human enzyme. Electron-donating substituents at C-5 (**12**, **13**) were disfavored and electron-withdrawing substituents favored (**14**, **15**) with respect to inhibition of PfNMT, but were accompanied by a drop in selectivity over human NMT. Changes at the C-6 position (**16**, **17**) were poorly tolerated.

Table 1.Enzyme activities of compounds with scaffold substitutions

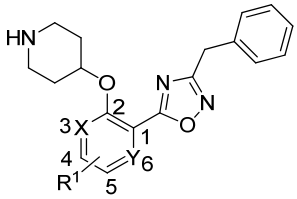

Compd no.	R^1	X	Y	PfNMT K_i (μM)[a]	HsNMT K_i (μM)[a]	S.I.[b]
3	H	CH	CH	1.4	34	24
4	3-OMe	C	CH	17	n.d.	-

5	3-Me	C	CH	39	n.d.	-
6	3-F	C	CH	1.5	15	10
7	H	N	CH	0.14	1.7	12
8	4-Me	CH	CH	0.62	44	70
9	4-OMe	CH	CH	0.18	1.2	6.8
10	4-F	CH	CH	0.22	4.9	22
11	4-Cl	CH	CH	0.29	17	58
12	5-Me	CH	CH	29	n.d.	-
13	5-OMe	CH	CH	4.6	2.3	0.5
14	5-F	CH	CH	0.24	1.0	4.0
15	5-Cl	CH	CH	0.52	0.73	1.4
16	6-F	CH	C	4.8	n.d.	-
17	H	CH	N	29	n.d.	-

[a] Apparent inhibitor dissociation constant K_i; Half maximal inhibitory concentration (IC_{50}) values were determined by a fluorogenic assay[30] and differences in substrate K_m accounted for using the Cheng–Prusoff equation to give a value for apparent K_i. [b]S.I. = selectivity index, calculated as apparent K_i(HsNMT1)/apparent K_i(PfNMT).

3-OMe phenyl as the terminal aromatic moiety. Based on enzyme potency and S.I. values, cores from compounds **7**, **9**, **10** and **11** were selected for further development, and a terminal 3-OMe phenyl moiety was selected for incorporation via the oxadiazole linker, based on our previous work.[28] The corresponding compounds

19-**22** along with the unsubstituted phenyl analogue **18** were prepared and it was found that addition of a 3-methoxy group generally enhances PfNMT inhibition activity, although at the expense of some human selectivity (**19**-**22** in Table 2 vs. **7**, **9**, **10** and **11** in Table 1). Compound **19** was selected as the frontrunner inhibitor at this stage given its balance of good potency and selectivity; furthermore, its higher LipE value is attractive for further development.[31, 32]

Table 2.Biological activities of 3-OMe phenyl analogues **18**-**22**

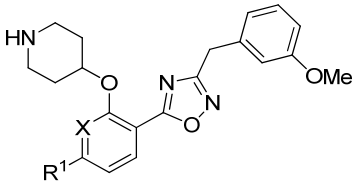

Compound	X	R^1	cLogP[a]	PfNMT K_i (μM)	HsNMT K_i (μM)	S.I.	LipE[b]
18	CH	H	3.40	0.19	1.4	7	3.32
19	N	H	2.79	0.027	0.27	10	4.78
20	CH	OMe	3.20	0.071	0.43	6.1	3.95
21	CH	F	3.54	0.071	0.54	7.6	3.61
22	CH	Cl	3.96	0.03	0.36	12	3.56

[a]cLogP calculated using ChemAxon software. [b] LipE = pKi (PfNMT) - cLogP.

Structural studies. *P. vivax* (Pv) NMT shares 81% sequence identity with PfNMT, and has been successfully used to guide the discovery of potent PfNMT inhibitors.[26-28] In order to interpret the effect of substitution on the scaffold, inhibitors derived from phenyl (**18**), 4-chloro phenyl (**22**) and 3-pyridyl (**19**) were selected for crystallographic studies and co-crystal structures with a non-hydrolysable

myr-CoA analogue (NHM)[30] and PvNMT were obtained. As expected, inhibitor **18** shows a very similar binding mode to a previously reported inhibitor **23** (Figure 2a).[28] Surprisingly, electron density maps suggest the formation of a ring-open analogue of the oxadiazole for these three test compounds within the crystal (the corresponding analogue for **18** is shown in Figure 2b), although the desired closed ring was confirmed for the pure isolated inhibitors by both NMR and high resolution mass spectrometry ($[M+H]^+$=366.1801, which matches well with its closed ring form), and they were found to be stable under conditions covering a pH range between 1 and 10 (data not shown). This interesting phenomenon was also observed in the related series crystallised in LmNMT,[29] and further work will be required to understand its origin; however, it did not impact on our subsequent development of the oxadiazole series. The basic piperidine moiety establishes an ion-pairing interaction with the C-terminal carboxylate (L410) and a cation-dipole interaction with the Y107 hydroxyl, whilst the 3-OMe phenyl forms hydrogen bonding (HB) and π-π interactions with the S319 hydroxyl and F105, respectively (Figure 2a). The 1,2,4-oxadiazole moiety is sandwiched between Y334 and Y211, forming hydrophobic interactions with these two residues. The observed substitution effects of the core can be clarified by examination of the bound structures (Figure 2c). Pyridyl **19** is superimposed with phenyl **18**, where the pyridyl nitrogen participates in an additional water-mediated HB with the Y315 hydroxyl, providing an explanation for the observed 8-fold enhancement in inhibition (**19** vs. **18**, Table 2). 4-Cl in **22** inserts into a hydrophobic

pocket formed by N365, A366 and L367; we hypothesise that such hydrophobic interaction provides the observed activity improvement (**22** vs. **18**, Table 2).

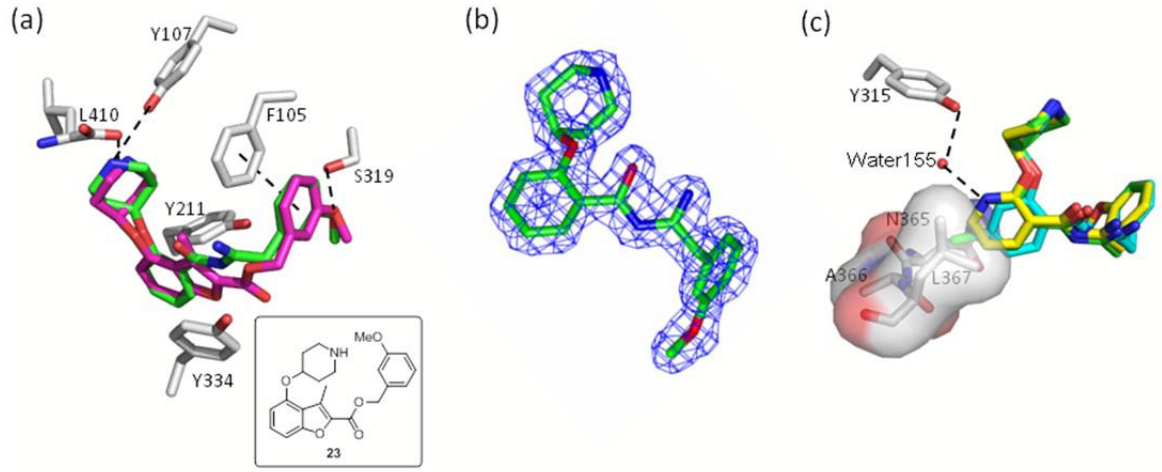

Figure 2. Structural overlays help to rationalize the SAR for **18**, **19** and **23**: (a) **18** (PDB code: 4UFV, 1.80 Å, green) binds to the enzyme (grey) in a similar way to **23** (PDB code: 4B14, magenta); (b) unexpected ring-open oxadiazole observed in the electron density map of **18** (C green); (c) **19** (PDB code: 4UFX, 1.51 Å, yellow) picks up an additional water-mediated hydrogen bond and shares identical binding positions to **18** (green); while insertion of chlorine at *C*-4 allows the hydrophobic interaction with the pocket comprising of N365, A366 and L367 (**22**, PDB code: 4UFW, 1.54 Å, cyan). Atoms are colored: N blue, O (non-water) red, O (water) red sphere.

Structure-guided development. We next considered replacements for the 3-OMe phenyl moiety. A structural overlay with **24**, a previously reported Pv/Pf NMT inhibitor,[26] suggests that the 1,3,5-trimethylpyrazole shares a similar binding mode to methoxyphenyl (Figure 3a). Pyrazole **25** was thus prepared (Scheme 2). Although it showed higher LipE than **19**, there was no potency boost in either enzyme or cellular

level while its *N*-alkyl piperidine derivatives (**26**-**28**) suffered from modest to significant activity drop (Table 3). Another PvNMT inhibitor (**29**) identified from an earlier screening campaign,[23] was found to overlay well with the 3-OMe phenyl moiety in **19** (Figure 3b). Encouragingly, the combination of quinoline and pyridyl scaffold yielded inhibitor **30** (Scheme 3), which posted a 14-fold increase in both enzyme and cellular potency over **19**, with only two heavy atoms added and no compromise in enzyme selectivity over human NMT or acute toxicity against mammalian cells over 48 hours (**30** vs. **19**, Table 3). We hypothesise that the improved HB acceptor strength of the quinoline[33] contributes to the observed increase in activity.

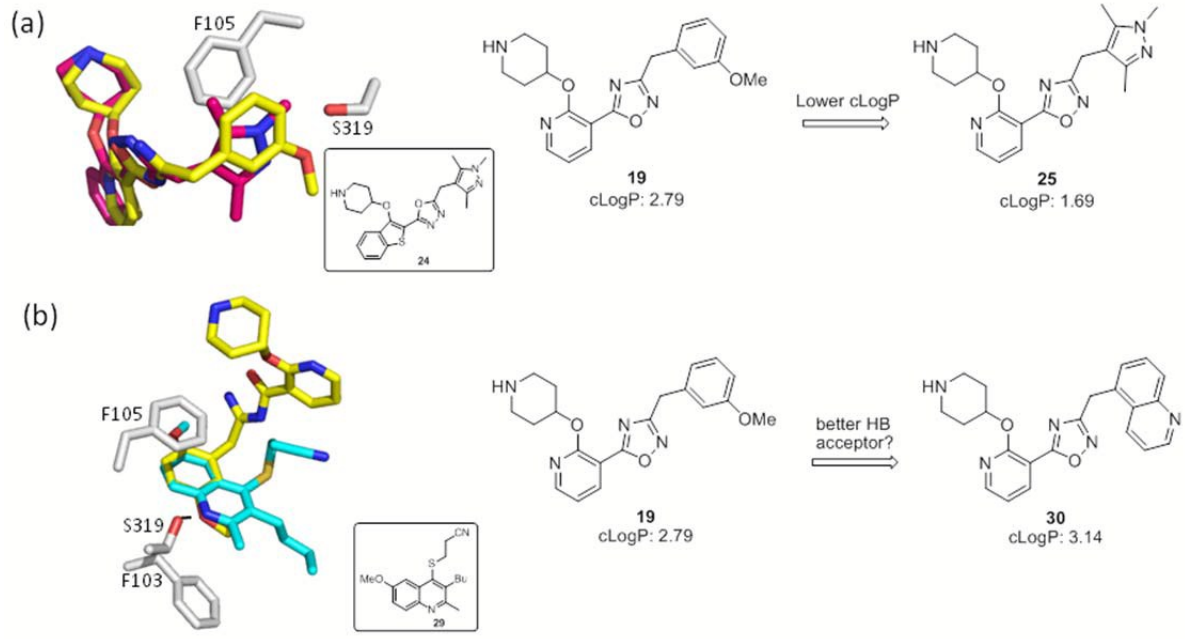

Figure 3. Structure-guided design: (a) overlay of 3-OMe phenyl in **19** (PDB code: 4UFX, yellow) with the pyrazole in **24** (PDB code: 4CAF, magenta). Both motifs bind at the S319 pocket; (b) 3-OMe phenyl in **19** superimposes well with the

quinoline in **29** (PDB code: 4A95, cyan). Atoms are colored: C (enzyme) grey, N blue, O red, S orange

Scheme 2[a]

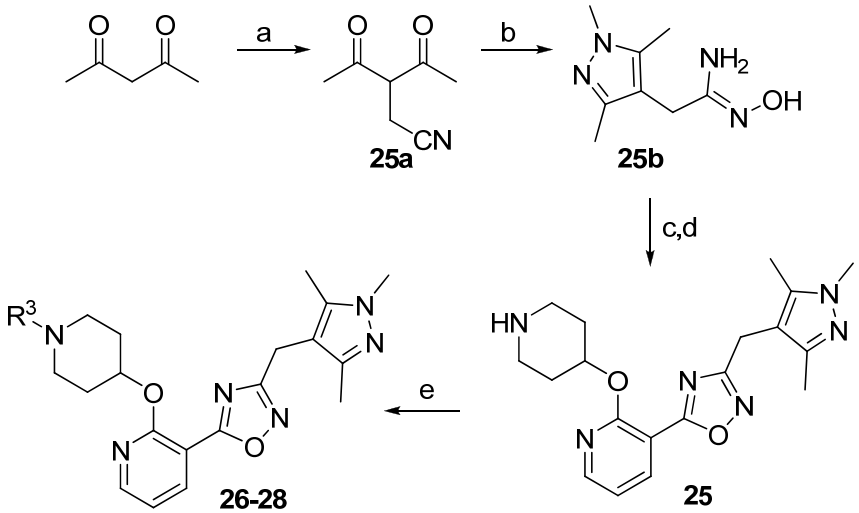

[a]Reagents: (a)bromoacetonitrile, NaH, THF, rt, 4 h, 40%; (b) i) mono-methylhydrazine, MeOH, reflux, 4 h; ii) hydroxylamine, MeOH, reflux, 6 h, 95%; (c) i). **7b**, EDCI, HOBt, DIPEA, CH_3CN, rt, 4 h; ii). 0.5N NaOH, rt, 0.5h, 90%; (d) 10% TFA in DCM (v/v), rt, 2 h, quantitative. (e) aldehyde or ketone, $NaBH(OAc)_3$, MeOH, rt, 12 h, 80%.

Scheme 3[a]

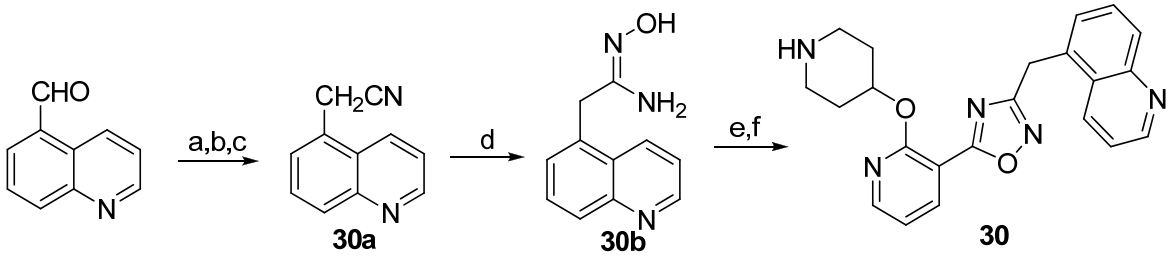

[a]Reagents: (a) $NaBH_4$, MeOH, rt, 8 h; (b) MsCl, DCM, 0 ºC, 3h; (c) NaCN, DMSO , 60 ºC, 1h, 22% over three steps; (d) hydroxylamine, MeOH, reflux, 6 h, 97%; (e) i). **7b**, EDCI, HOBt, DIPEA, CH_3CN, rt, 4 h; ii). 0.5N NaOH, rt, 0.5h, 90%; (f) 10% TFA in DCM (v/v), rt, 2 h, quantitative.

Table 3. Biological activities of inhibitors guided by overlaying crystal structures

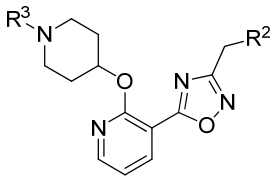

Compd no.	R^2	R^3	cLogP[a]	PfNMT K_i (μM)	LipE[b]	HsNMT K_i (μM)	S.I.[c]	EC_{50} (μM)[d]	LD_{50} (μM)[e]
19	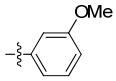	H	2.79	0.027	4.78	0.27	10	3.5	70
25	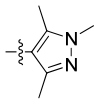	H	1.69	0.028	5.86	0.20	7	3.7	>100
26	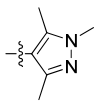	Me	2.09	0.57	4.15	0.51	0.9	>30	n.d.[f]
27	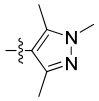	Et	2.44	0.34	4.03	0.27	0.8	>10	n.d.
28	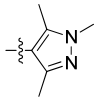	*i*-Pr	2.85	0.090	4.20	0.18	2	3.2	>100
30	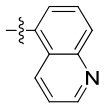	H	3.14	0.0017	5.63	0.024	14	0.21	65

[a] cLogP values calculated using ChemAxon software. [b] LipE = pKi (PfNMT) – cLogP; [c]S.I., calculated as K_i(HsNMT1)/K_i(PfNMT). [d] *P. falciparum*, 3D7 line was used; [e] HepG2 cell line was used; [f] n.d. = not detected.

CONCLUSION

Scaffold reduction from our earlier PfNMT inhibitors containing bicyclic cores to phenyl-based inhibitors provided a flexible platform to study the effect of scaffold and substituent variations, allowing the discovery of pyridyl as an attractive core, the superiority of which was later explained by co-crystallography. Further development was achieved through crystallography-guided hybridization of this scaffold with two existing NMT inhibitors, leading to the discovery of **30**, a promising PfNMT inhibitor with excellent enzyme affinity and good cellular efficacy. Further lead optimization is underway in an attempt to further improve the cellular potency of this series, with the aim of progressing towards *in vivo* studies.

ASSOCIATED CONTENT

Supporting Information Available. Experimental procedures and characterization of all intermediates, target compounds and X-Ray crystallographic data. The coordinates and structure factor files have been deposited in the Protein Data Bank under the accession codes 4UFV (PvNMT-NHM-18), 4UFW (PvNMT-NHM-22) and 4UFX (PvNMT-NHM-19).

AUTHOR INFORMATION

Corresponding Authors

* EWT Phone: +44 2075 943 752. Email: e. tate@imperial.ac.uk

ACKNOWLEDGEMENTS

This work was supported by the Wellcome Trust (grant number: 087792), the Medical Research Council (grant numbers: 0900278 and U117532067) and the Francis Crick Institute which receives its core funding from Cancer Research UK, the UK Medical Research Council and the Wellcome Trust. The authors are grateful to Andrew Bell, Mark Rackham and Jennie Hutton for valuable discussions. We thank Munira Grainger for providing the parasites and red blood cells used in the *in vitro* parasite assay, Shirley Roberts for crystal handling and Johan Turkenburg for X-ray data processing. We also acknowledge the Diamond Light Source for Synchrotron facilities.

REFERENCES

1. *World Malaria Report 2014*. 2014, Geneva: World Health Organization
2. The RTS, S.C.T.P., *N. Engl. J. Med.*, 2012, **367**, 2284.
3. A. Opar , *Nat. Rev. Drug Discov.*, 2011, **10**, 887.
4. J. Straimer, N.F. Gnadig, B. Witkowski, C. Amaratunga, V. Duru, A.P. Ramadani, M. Dacheux, N. Khim, L. Zhang, S. Lam, P.D. Gregory, F.D. Urnov, O. Mercereau-Puijalon, F. Benoit-Vical, R.M. Fairhurst, D. Menard and D.A. Fidock, *Science*, 2015, **347**, 428.
5. A.P. Phyo, S. Nkhoma, K. Stepniewska, E.A. Ashley, S. Nair, R. McGready, C. ler Moo, S. Al-Saai, A.M. Dondorp, K.M. Lwin, P. Singhasivanon, N.P.J. Day, N.J. White, T.J.C. Anderson and F. Nosten, *Lancet*, 2012, **379**, 1960.
6. A.M. Dondorp, F. Nosten, P. Yi and D. Das, *N. Engl. J. Med.*, 2009, **361**, 455.

7. J.N. Burrows, E. Burlot, B. Campo, S. Cherbuin, S. Jeanneret, D. Leroy, T. Spangenberg, D. Waterson, T.N. Wells and P. Willis, *Parasitology*, 2014, **141**(Special Issue 01), 128.
8. E.W. Tate, K.A. Kalesh, T. Lanyon-Hogg, E.M. Storck, and E. Thinon, *Curr. Opin. Chem. Biol.*, 2015, **24**, 48.
9. E. Thinon, R.A. Serwa, M. Broncel, J.A. Brannigan, U. Brassat, M.H. Wright, W.P. Heal, A.J. Wilkinson, D.J. Mann and E.W. Tate, *Nat. Commun.*, 2014, **5**.
10. E.W. Tate, A.S. Bell, M.D. Rackham and M.H. Wright, *Parasitology*, 2013, **FirstView**, 1.
11. M. Wright, W. Heal, D. Mann and E. Tate, *J. Chem. Biol.*, 2010, **3**, 19.
12. D.R. Johnson, R.S. Bhatnagar, L.J. Knoll and J.I. Gordon, *Annu. Rev. Biochem.*, 1994, **63**, 869.
13. D. Guttery, S. Poulin, B. Ramaprasad, A. Wall, R.J. Ferguson, D.J.P. Brady, D. Patzewitz, E.M. Whipple, S. Straschil, M.H. Wright, A. Mohamed, M.A.H. Radhakrishnan, A.S.T. Arold, E.W. Tate, A.A. Holder, B. Wickstead, A. Pain and R. Tewari, *Cell host & microbe*, 2014, **16**, 128.
14. B. Poulin, E.M. Patzewitz, D. Brady, O. Silvie, M.H. Wright, D.J.P. Ferguson, R.J. Wall, S. Whipple, D.S. Guttery, E.W. Tate, B. Wickstead, A.A. Holder and R. Tewari, *Biol. Open*, 2013, **2**, 1160.
15. W. Leber, A. Skippen, Q.L. Fivelman, P.W. Bowyer, S. Cockcroft and D.A. Baker, *Int. J. Parasitol.*, 2009, **39**, 645.
16. J.L. Green, R.R. Rees-Channer, S.A. Howell, S.R. Martin, E. Knuepfer, H.M. Taylor, M. Grainger and A.A. Holder, *J. Biol. Chem.*, 2008, **283**, 30980.
17. R.R. Rees-Channer, S.R. Martin, J.L. Green, P.W. Bowyer, M. Grainger, J.E. Molloy and A.A. Holder, *Mol. Biochem. Parasitol.*, 2006, **149**, 113.
18. W.H.L. Stafford, R.W. Stockley, S.B. Ludbrook and A.A. Holder, *Eur. J. Biochem.*, 1996, **242**, 104.
19. M.H. Wright, B. Clough, M.D. Rackham, K. Rangachari, J.A. Brannigan, M. Grainger, D.K. Moss, A.R. Bottrill, W.P. Heal, M. Broncel, R.A. Serwa, D. Brady, D.J. Mann, R.J. Leatherbarrow, R. Tewari, A.J. Wilkinson, A.A. Holder and E.W. Tate, *Nat. Chem.*, 2014, **6**, 112.
20. P. Pino, S. Sebastian, E.A. Kim, E. Bush, M. Brochet, K. Volkmann, E. Kozlowski, M. Llinas, O. Billker and D. Soldati-Favre, *Cell host & microbe*, 2012, **12**, 824.
21. J.A. Hutton, V. Goncalves, J.A. Brannigan, D. Paape, M.H. Wright, T.M. Waugh, S.M. Roberts, A.S. Bell, A.J. Wilkinson, D.F. Smith, R.J. Leatherbarrow and E.W. Tate, *J. Med. Chem.*, 2014, **57**, 8664.
22. J.A. Brannigan, S.M. Roberts, A.S. Bell, J.A. Hutton, M.R. Hodgkinson, E.W. Tate, R.J. Leatherbarrow, D.F. Smith and A.J. Wilkinson, *IUCrJ*, 2014, **1**, 250.
23. V. Goncalves, J.A. Brannigan, D. Whalley, K.H. Ansell, B. Saxty, A.A. Holder, A.J. Wilkinson, E.W. Tate and R.J. Leatherbarrow, *J. Med. Chem.*, 2012, **55**, 3578.

24. A.S. Bell, J.E. Mills, G.P. Williams, J.A. Brannigan, A.J. Wilkinson, T. Parkinson, R.J. Leatherbarrow, E.W. Tate, A.A. Holder and D.F. Smith, *PLoS Negl. Trop. Dis.*, 2012, **6**, e1625.
25. T.O. Olaleye, J.A. Brannigan, S.M. Roberts, R.J. Leatherbarrow, A.J. Wilkinson and E.W. Tate, *Org. Biomol. Chem.*, 2014, **12**, 8132.
26. M.D. Rackham, J.A. Brannigan, K. Rangachari, S. Meister, A.J. Wilkinson, A.A. Holder, R.J. Leatherbarrow and E.W. Tate, *J. Med. Chem.*, 2014, **57**, 2773.
27. M.D. Rackham, J.A. Brannigan, D.K. Moss, Z. Yu, A.J. Wilkinson, A.A. Holder, E.W. Tate and R.J. Leatherbarrow, *J. Med. Chem.*, 2013, **56**, 371.
28. Z. Yu, J.A. Brannigan, D.K. Moss, A.M. Brzozowski, A.J. Wilkinson, A.A. Holder, E.W. Tate and R.J. Leatherbarrow, *J. Med. Chem.*, 2012, **55**, 8879.
29. M.D. Rackham, Z. Yu, J.A. Brannigan, W.P. Heal, D. Pappe, K.V. Barker, A.J. Wilkinson, D.F. Smith, R.J. Leatherbarrow and E.W. Tate, *MedChemComm*, submitted.
30. V. Goncalves, J.A. Brannigan, E. Thinon, T.O. Olaleye, R. Serwa, S. Lanzarone, A.J. Wilkinson, E.W. Tate and R.J. Leatherbarrow, *Ana. Biochem.*, 2012, **421**, 342.
31. A.L. Hopkins, G.M. Keseru, P.D. Leeson, D.C. Rees and C.H. Reynolds, *Nat. Rev. Drug Discov.*, 2014, **13**, 105.
32. A. Tarcsay, K. Nyiri and G.M. Keseru, *J. Med. Chem.*, 2012, **55**, 1252.
33. H.J. Böhm, S. Brode, U. Hesse and G. Klebe, *Chem. Eur. J.*, 1996, **2**, 1509.